A superconducting dual-channel photonic switch

Srivastava, Yogesh Kumar; Manjappa, Manukumara; Cong, Longqing; Krishnamoorthy, Harish N. S.; Savinov, Vassili; Pitchappa, Prakash; Singh, Ranjan

2018

Srivastava, Y. K., Manjappa, M., Cong, L., Krishnamoorthy, H. N. S., Savinov, V., Pitchappa, P., & Singh, R. (2018). A superconducting dual-channel photonic switch. Advanced Materials, 30(29), 1801257-. doi:10.1002/adma.201801257

https://hdl.handle.net/10356/137405

https://doi.org/10.1002/adma.201801257

Superconducting dual-channel photonic switch

Yogesh Kumar Srivastava[1,2], *Manukumara Manjappa*[1,2], *Longqing Cong*[1,2], *Harish N. S. Krishnamoorthy*[1,2], *Vassili Savinov*[3], *Prakash Pitchappa*[1,2], *and Ranjan Singh*[1,2,*]

Yogesh Kumar Srivastava, Manukumara Manjappa, Dr. Longqing Cong, Dr. Harish N. S. Krishnamoorthy, Dr. Vassili Savinov, Dr. Prakash Pitchappa and Prof. Ranjan Singh

[1]Division of Physics and Applied Physics, School of Physical and Mathematical Sciences, Nanyang Technological University, 21 Nanyang Link, Singapore 637371, Singapore

[2]Center for Disruptive Photonic Technologies, The Photonics Institute, Nanyang Technological University, 50 Nanyang Avenue, Singapore 639798, Singapore

[3]Optoelectronics Research Centre and Centre for Photonic Metamaterials, University of Southampton, Southampton, SO17 1BJ, United Kingdom

*E-mail: ranjans@ntu.edu.sg

Keywords: dual channel switching, ultrafast dynamics, high-temperature superconductors, terahertz metamaterials, YBCO

Abstract:

The mechanism of Cooper pair formation and underlying physics has long occupied the investigation into high temperature (high-T_c) cuprate superconductors. One of the ways to unravel this is to observe ultrafast response present in charge carrier dynamics of a photoexcited specimen. This results in an interesting approach to exploit the dissipation-less dynamic features of superconductors to be utilized for designing subwavelength photonic devices with extremely low-loss operation. Here, we experimentally demonstrate dual-channel, ultrafast, all-optical switching and modulation between the resistive and the superconducting quantum mechanical phase. The ultrafast phase switching is demonstrated via modulation of sharp Fano resonance of a high-T_c Yttrium Barium Copper Oxide (YBCO) superconducting metamaterial device. Upon

photoexcitation by femtosecond light pulses, the ultrasensitive cuprate superconductor undergoes dual dissociation-relaxation dynamics, with restoration of superconductivity within a cycle, and thereby establishes the existence of dual switching windows within a timescale of 80 ps. We explored pathways to engineer the secondary dissociation channel which provides unprecedented control over the switching speed. Most importantly, our results envision new ways to accomplish low-loss, ultrafast and ultrasensitive dual channel switching applications that are inaccessible through conventional metallic and dielectric based metamaterials.

Introduction:

Superconductors are a fascinating family of materials, typically characterized by vanishing electrical resistance and perfect diamagnetism below a certain critical temperature (T_c). Superconductors have enabled important applications in several fields such as in high power electromagnets, magnetic resonance imaging (MRI) machines, nuclear magnetic resonance (NMR) spectrometers, highly sensitive magnetometers and frictionless magnetic levitation devices. The discovery of high-T_c superconductors (HTS) has given a major impetus to the technological advancement of these devices, as the superconductivity in HTS materials could be achieved above liquid nitrogen temperature.[1-2] They are efficient electrical conductors with negligible loss below the T_c and behave as poor metals above T_c. When HTS material is cooled below T_c, charge carriers pair up to form Cooper pairs and the extraordinary conductivity of superconductors is attributed to the presence of a superfluid (Cooper pairs).[3-4] At and above T_c, Cooper pairs cease to exist and behave as normal quasiparticles. The binding energy of Cooper pairs in HTS is typically in the range of 2-75 meV, [3-5] which makes terahertz frequency spectrum an ideal tool to investigate the transient dynamics of Cooper pairs in superconductors. Superconductivity is highly sensitive to the energy of the incident photon greater than the binding energies of the Cooper pairs. When irradiated, Cooper pairs dissociate and recombine in extremely short timescale of few picoseconds (ps).[6-9] During this process, there is a significant reduction in the density of Cooper pairs leading to a drastic decrease in the conductivity of the superconductor, thereby resulting in an ultrafast switching from an excellent electrical conductor to a poor metal. This active dissociation and recombination of Cooper pairs at such short timescale make superconductors an excellent macroscopic quantum material platform for enhanced THz radiation generation[10-11] and high-speed switching applications in photonics.

Metamaterials offer unique opportunities based on their structural geometry to precisely manipulate light-matter interactions and have been used to demonstrate several exotic phenomena such as flat lens, subwavelength imaging, slowing and trapping of light pulses, perfect absorption and chirality.[12-18] Superconductors are proposed and widely used for the realization of low-loss metamaterials by curbing ohmic losses due to their extraordinary conducting properties at radio frequency, microwave and terahertz frequency regimes.[19-23] Incorporating superconductors in metamaterial structures also enable active control of optical response as the conducting properties of superconductors are highly sensitive to the external stimuli. This has led to the realization of actively tunable superconducting metadevices using perturbations such as magnetic field[24-26], temperature[20, 27-29], electrical current[30-32] and optical excitation[9]. However, the change in optical response brought about by thermal perturbation is quite slow, while employing electrical perturbation requires careful considerations into design and fabrication. Active control of meta-device response at ultrafast timescale is a highly desirable feature for realizing dynamically tunable state-of-the-art devices for on-demand applications. Hence, optical control of high-T_c superconductor based metamaterials is an ideal approach for the realization of ultrafast terahertz photonic devices.

Here, we experimentally demonstrate the ultrafast switching of Fano resonance[33-34] by optical pumping of high-T_c YBCO superconductor based terahertz asymmetric split ring (YBCO-TASR) metamaterial. Upon pumping with optical pulse of energy much higher than the binding energy of Cooper pairs, the primary dissociation occurs due to the breaking of superconducting Cooper pairs into quasiparticles. These quasiparticles recombine to form quantum mechanical superconducting Cooper pairs in picoseconds (ps) timescale.[6-7] Interestingly, the Fabry-Perot etalon pulse from the substrate leads to the secondary dissociation of the Cooper pairs. The ultrasensitive nature of Fano

resonance[33-36] allows for the observation of the resonance modulation even for the secondary dissociation in the photoexcited superconductor metamaterial, which was inaccessible in the earlier reported highly radiative inductive-capacitive (LC) superconductor resonator system.[9] Upon photoexcitation with high fluence of optical pump, the Fano resonant metadevice show existence of dual switching windows with different time constants due to the dual dissociation-relaxation of Cooper pairs within a complete restoration cycle of superconductivity. Such dual channel ultrafast switching behavior is inaccessible through conventional metallic and dielectric based metamaterials. In addition to the ultrafast modulation, we also show that similar modulation could be achieved at much larger timescale by tuning the temperature of the YBCO-TASR. Actively tunable high-Q resonances are highly desirable for applications such as ultrasensitive sensing, slow light, nonlinearity, acoustic coding and manipulation of light propagation.[16, 37-49]

Discussion:

To enable active control of sharp Fano resonance using photoexcitation and temperature tuning, we choose terahertz asymmetric split ring (TASR) metamaterial design, as schematically shown in Figure 1(a). The TASR is primarily a double-gap asymmetric split ring resonator, where asymmetry in the structure is introduced by displacing one of the capacitive gaps away from the central vertical axis by a distance 'd'. In such TASR structures, Fano resonance is excited by the electric field of terahertz wave polarized (E_x) perpendicular to the gap side arms of the resonator, which also results in a broad dipolar resonance mode at a higher frequency.[51] The observed Fano resonance feature is due to the interference between the broad dipole (bright) mode of the perfectly symmetric structure and a narrow discrete (dark) mode arising from the break in the structural symmetry.[50-52] In the present case, an asymmetry of $d = 15$ μm is chosen to get a resonant response of high amplitude for the ease of capturing the spectral footprint in the measurements. However,

ultra-high Q resonators can be readily designed by decreasing the asymmetry parameter (d) value.[51-52] The metamaterial sample was fabricated using photolithography and wet etching of 50 nm thick YBCO film on 500 μm thick *r*-cut sapphire substrate. Details of the fabrication process are given in the experimental method section. Optical image of the fabricated YBCO-TASR is shown in Figure 1(b) and the inset shows the TASR unit cell with geometrical parameter definitions. The terahertz transmission spectra of the metamaterial were measured at various temperatures ranging from 5 K to 295 K using a ZnTe crystal based confocal terahertz time-domain spectroscopy system. The system was incorporated with a continuous flow liquid helium cryostat to facilitate measurements at cryogenic temperatures. The measurement details are given in the experimental method section.

The Cooper pairs are readily dissociated by photoexcitation of the superconducting film with optical fields of frequencies above the binding energy of the Cooper pairs and alter the conducting properties that show strong influence on the resonance properties of the metadevices. The terahertz transmission spectra of the YBCO-TASR under the influence of photoexcitation were measured using an optical-pump and terahertz-probe (OPTP) spectroscopy setup (described in the experimental method section). In the measurement of the pump dependent terahertz transmission spectra, the terahertz pulse was delayed by 4.9 ps (the rise time of Cooper pair dissociation dynamics) with respect to pump pulse, so that we obtain the maximum dissociation of Cooper pairs. Figure 2(a) shows the terahertz transmission response of the YBCO-TASR for different fluences of optical excitation pulses, which is defined as radiant energy per unit surface area (μJ/cm^2). When the fluence of the optical pump is low (~63.7 μJ/cm^2), a weak modulation of the Fano and dipole resonances are observed. As the incident pump fluence is increased, a larger reduction in the Fano and dipole resonance amplitude is observed. This reduction in the Fano and

dipole resonance amplitude is attributed to the reduced density of Cooper pairs. The optical excitation pulse destroys a fraction of Cooper pairs into quasiparticles, thereby resulting in the reduced overall conductivity of YBCO. The percentage of Cooper pairs that dissociated into quasiparticles is strongly dependent on the fluence of the incident optical excitation pulse. At a pump fluence of 955.4 μJ/cm^2, the Fano and dipole resonances are significantly reduced due to the breaking up of a large fraction of Cooper pairs in YBCO. However, the resonances are not completely switched off at this pump fluence due to the existence of a relatively smaller fraction of remnant Cooper pairs. The percentage amplitude modulation of Fano and dipole resonances at different excitation pulse fluences were calculated as $(T_{off}-T_{on})/T_{off} \times 100$ %, where T_{off} and T_{on}, respectively, stands for the transmission resonance amplitudes during 'off' and 'on' states of the optical pump beam. The transmission resonance amplitude is the difference between the peak and dip of the resonance in the transmission spectra. The experimentally measured percentage amplitude modulation depths of Fano and dipole resonances are shown in Figure 2(b). The maximum value of amplitude modulation was observed to be 86% for Fano resonance and 60% for dipole resonance, respectively. The Fano resonance depicts higher sensitivity to the optical pump at similar pump fluences in comparison to the dipole resonance, owing to the strong field confinement in the capacitive gaps of the resonator at Fano resonant frequency. It can be noticed that a relatively large pump fluence is required to switch off the Fano and dipole resonances in a 50 nm thick YBCO-TASR sample. However, further engineering of the sample with reduced sample thickness can potentially provide a significant reduction in the optical fluences to achieve a complete low threshold switching performance. In our sample, the active resonator area which is the fill fraction of superconductor is less than 23% of the entire metamaterial area. Focusing the excitation pulse onto the superconducting area, which can be achieved by structuring the back-

side of the sapphire substrate, could also significantly reduce the optical pump fluence required for complete switching.[53-54]

Further, we capitalize on the ultrafast behavior observed in the dissociation and recombination of the Cooper pairs in the YBCO superconductor that occurs at picoseconds timescale to demonstrate ultrafast modulation of Fano resonance in the YBCO-TASR sample. The black line in Figure 3(a) shows the charge carrier dynamics of the YBCO-TASR sample (fabricated on 500 μm thick sapphire substrate), at 5 K under the illumination of the optical pump pulse of 800 nm wavelength with fluence of 254.8 μJ/cm^2. As the sample is illuminated by the optical pump pulse of energy greater than the dissociation energy of the Cooper pairs, the superconductivity is destroyed by breaking the Cooper pairs momentarily. This sudden dramatic reduction in the conductivity leads to an increase in the differential terahertz transmission signal. After few picoseconds, the quasiparticles bind together to form Cooper pairs again and thus the superconductivity is restored. We also note that a secondary peak evolves gradually at the time delay of around 6 ps from the primary dissociation peak in the excitation dynamics. The evolution of the secondary peak is due to the secondary dissociation of the Cooper pairs by reflected optical pulse approaching from the back surface of the substrate. The round trip time taken by the incident optical beam of wavelength 800 nm before resulting in secondary dissociation is given as $2nt_s/c$, where n is the refractive index of the substrate material at optical pump wavelength, t_s is the substrate thickness and c is the speed of light in vacuum. For a 500 μm thick sapphire substrate with refractive index of 1.76 at 800 nm, the reflected pulse from the back surface of the substrate is delayed by 5.9 ps, which matches closely with the experimentally observed delay. The secondary peak could be engineered by altering optical reflection from the back surface of the substrate by changing the substrate properties such as thickness (t_s) or refractive index (n) and provides an interesting way to

manipulate the switching speed of the metamaterial device. The red dashed line in Figure 3(a) depicts the charge carrier dynamics of the YBCO-TASR fabricated over a 2 mm thick sapphire substrate under the illumination of the identical optical pump fluences. We observed that the secondary excitation peak is delayed by 23.6 ps from the primary excitation peak, which closely matches with the calculated time delay of 23.4 ps for 2 mm thick sapphire substrate. It is important to note that the THz probe pulse will experience similar Fabry-Perot reflections from the back surface of substrate but there would not be any effect on the charge carrier dynamics due to the reflected THz pulse. This is due to the fact that the THz probe pulse (0.4-8.2 meV) will not disossociate the Cooper pairs as its energy is lower than the binding energy of the Cooper pairs in YBCO (20-30 meV).[3-5]

The ultrafast response of the Cooper pair recombination dynamics of the superconductor is reflected in the resonance transmission characteristics of the YBCO-TASR sample. Figure 3(b) represents the ultrafast modulation in the terahertz transmission spectra of the superconducting YBCO-TASR sample at different time delay, τ_p marked as A, B, C and D of the optical pump pulse depicted in Figure 3(a). At point A, just before (τ_p = -2 ps) the optical excitation, the Fano resonance strength at 0.40 THz is very strong and is shown by the black curve in Figure 3(b). At point B (τ_p = 4.9 ps), where the dissociation of Cooper pairs is maximum, the Fano resonance shows a strong reduction in its resonance strength owing to the significant decrease in the imaginary part of the complex conductivity of the YBCO film. These dissociated Cooper pairs bind together again to recover superconductivity, which results in a gradual increase in the strength of Fano resonance amplitude at C (τ_p = 9.2 ps) and D (τ_p = 38.3 ps). Here, it is worth mentioning that, there is a trade-off between the excitation pump fluence and the ultrafast response of the sample. High pump fluences result in large modulation depth but slow switching speed, whereas

low pump fluences result in lower modulation depth but faster switching speed. Hence, to obtain both appreciable modulation depths and ultrafast optical response from the sample, we chose to pump the sample with fluence of 254.8 $\mu J/cm^2$. This results in partial modulation of 44% in the amplitude of the Fano resonance at the maximum dissociation point (B) of Cooper pairs, which can be restored within 40 ps. We also note that the resonance is not completely restored due to the thermal effects from local heating of the sample by the incident optical pump beam.

To capture the secondary dissociation footprints in the Fano resonances feature, we measured the terahertz transmission response at various time delays (τ_p) between pump and probe varied in small steps. Figure 3(c) depicts the percentage modulation of Fano resonance amplitude at varying time delay between optical pump and terahertz probe pulses. We observed that initially the modulation in the resonance amplitude increases rapidly and attains a maximum value at $\tau_p = 4.9$ ps due to maximum degree of dissociation of the Cooper pairs. The modulation in the resonance amplitude starts reducing with further increase in the time delay till the reflected pulse hits the sample at $\tau_p =$ 10.7 ps. We observe a clear peak in the modulation of amplitude transmission at $\tau_p = 10.7$ ps (highlighted in red circle) which is due to the secondary dissociation of the Cooper pairs that arises from the Fabry-Perot reflected optical pulse approaching from the back surface of the substrate. The percentage amplitude modulation decreases gradually upon further increase in the time delay. Here, the extreme sensitivity of Fano resonance feature to the changes in conductivity of the superfluidpaves the way to experimentally observe the dual dissociation-relaxation window within a single superconductivity restoration cycle and to realize the dual channel meta-switch.

To estimate the recovery time of the dissociated Cooper pairs, we analyzed the charge carrier dynamics of YBCO-TASR sample for varying optical pump fluences. Figure 4(a), 4(b) and 4(c) show the normalized charge carrier dynamics of the YBCO-TASR sample at 5 K measured using

the OPTP setup at the excitation pump fluences of 63.7, 127.4 and 254.8 μJ/cm^2, respectively. For the optical excitation pump fluence of 63.7 μJ/cm^2, only the primary dissociation is observed, whereas for higher pump fluences of 127.4 and 254.8 μJ/cm^2, an additional secondary dissociation is clearly seen along with the primary dissociation. Both the primary and secondary dissociation-relaxation dynamics follows bi-exponential relaxation as follows,

$$y = y_0 + A_1 e^{(-\frac{(x-x_0)}{t_1})} + A_2 e^{(-\frac{(x-x_0)}{t_2})} \quad (1)$$

where t_1 and t_2 reflects the lifetime of fast and slow relaxation processes, respectively. Even though the exact nature of the carrier dynamics of cuprate superconductors is not fully understood, the current consensus is that the fast relaxation time (t_1) is attributed to electronic transitions, which include relaxation of hot quasiparticles by breaking more Cooper pairs in the vicinity and electron-phonon (e-ph) mediated relaxation, while the slow relaxation time (t_2) is attributed to Cooper pair formation mediated by 2Δ phonons, where 2Δ is the superconducting energy gap.[55] At sufficiently low fluences of optical excitation, only a small fraction of Cooper pairs is directly excited into hot quasiparticles by incident photons and thus the hot quasiparticles relax to superconducting gap edge by interacting with a large fraction of the remnant Cooper pairs. However, at higher pump fluences, a large fraction of Cooper pairs is directly dissociated into hot quasiparticles thereby the relaxation process is dominated by e-ph interaction due to unavailability of sufficient remnant Cooper pairs required for relaxation of all hot quasiparticles to the superconducting gap edge. Hence at low pump fluences, the electronic transitions are dominated by relaxation of hot quasiparticles by breaking more Cooper pairs in the vicinity and at high pump fluence, it is dominated by e-ph mediated relaxation process. Once all the hot quasiparticles relaxes to the superconducting gap edge, they begin to form the Cooper pairs by emitting phonons of energy

equal to or greater than 2Δ. These emitted 2Δ phonons are capable of breaking Cooper pairs again, making the entire relaxation process slow. Finally, the phonons dissipate via diffusion into the substrate or by decaying into lower energy phonons thereby restoring the superconductivity. The extracted, fast and slow relaxation time constants for primary and secondary dissociation-relaxation dynamics at all the pump fluences are listed in the Table 1.

Table 1: Extracted relaxation time constants at different pump fluences

Pump fluence (μJ/cm^2)	Fitted time constants (ps)			
	Primary dissociation		Secondary dissociation	
	t_1	t_2	t_1'	t_2'
63.7	0.5	8.3	-	-
127.4	1.4	10.3	2.8	49.7
254.8	1.3	13.5	3.6	84.2

The bi-exponential fitting of primary dissociation (shown as red curves in Figure 4) reveals that the time constant of the faster decay is around 0.5-1.4 ps for all the pump fluences, whereas the relaxation timescale of the slower decay is around 8-13 ps. Similarly, the bi-exponential fitting of secondary dissociation reveals that the fast decay time constants are 2.8 and 3.6 ps, whereas the slow decay time constants are 49.7 and 84.2 ps for the pump fluences of 127.4 and 254.8 μJ/cm^2, respectively, as shown by the green curves in Figure 4(b) and 4(c). It can also be seen that with increasing pump fluences, the relaxation time increases which is caused due to the increased density of hot quasiparticles that results from the large dissociation of the Cooper pairs.[56] Even though the overall switching speed of the metadevice is determined by the slower time constants, the operational speed is still within 85 ps. Interestingly, the secondary peak in the charge carrier dynamics offers dual decay channels with different switching speeds of the resonances. This

peculiar feature of the secondary dissociation and switching speed control is due to the ultrasensitive nature of the Cooper pairs to the optical excitation. The two decay channels pave the path forward for dual switching speed with a single excitation fluence in such meta-devices. These designs could lay a useful platform for realizing ultrafast resonant modulators operating at terahertz and microwave frequencies.

Besides the optical control in the manipulation of the superconducting properties of YBCO, the Cooper pairs are extremely sensitive to the temperature. The thermal control of Fano resonance in superconducting YBCO-TASR metamaterials was characterized by varying the sample temperature. From Figure 5(a), we note that the spectra of YBCO-TASR show a very strong Fano and dipole resonance features at 5 K, which is due to the superconducting properties of YBCO well below the superconducting phase transition temperature. The amplitudes of the Fano and dipole resonance dimishes gradually as the temperature is increased from 5 K and finally disappears at 80 K, which is close to the superconducting phase transition temperature of the YBCO thin film. For temperature above 80 K, both the Fano and dipole resonance disappears completely due to the phase transition of YBCO into the normal state. This temperature dependent active on and off state of the YBCO-TASR is highly useful for active meta-devices. The temperature dependent response of the YBCO-TASR also induces red shifting of the Fano and dipole resonances with an increase in temperature due to the change in the kinetic inductance of the high-T_c superconducting YBCO.[57-58] A significant red shift of 80 GHz and 150 GHz is observed for the Fano and dipole resonances, respectively, by changing the temperature from 5 K to 70 K as shown in Figure 5(b). Modulation in the amplitude of the resonances is due to the reduction in the imaginary part of complex conductivity of the YBCO film due to the dissociation of a fraction of Cooper pairs into quasiparticles, whereas the observed spectral shift in the

resonance frequency is due to change in kinetic inductance of the Cooper pairs. This enables simultaneous control of Fano and dipole resonances in terms of amplitude modulation as well as the frequency tuning with the change in temperature.

In conclusion, we have experimentally demonstrated dual channel ultrafast modulation of Fano resonances upon photoexcitation by femtosecond near-infrared laser pulse that show resonance switching at extremely short timescale in a terahertz superconducting asymmetric split ring resonator metamaterial. We observed dual dissociation-relaxation dynamics in a single superconductivity restoration cycle which leads to the realization of the dual channel ultrafast meta-switch. Furthermore, we discussed an effective way to manipulate the secondary dissociation channel by changing the substrate properties, which provides a large control over the switching speed of the metadevices. These dual channel switchable devices could be highly useful for several applications such as time-division multiplexing, terahertz high speed wireless communication, superconducting radiation sensors and superconducting photodetectors. The ultrafast switchable nature of superconductors continues to attract great interest in low-loss, high speed photonics, nonlinear metamaterials/plasmonic devices and for understanding the macroscopic quantum phenomenon.

Experimental Method:

1- Sample Fabrication:

The metamaterial sample was fabricated using standard photolithography technique on a commercially available M-type YBCO film of thickness 50 nm deposited over a 500 μm thick sapphire substrate. This YBCO film has a superconducting transition temperature of 85.1 K and

critical current density of 2.9 MA/cm^2. The YBCO film was thoroughly cleaned using acetone and IPA, and dried with nitrogen gas. A positive photoresist of thickness 1.5 µm was spin-coated over YBCO film. This sample was prebaked at 105° C on a hotplate and exposed with UV illumination after proper mask alignment. The sample was then soaked in the developer solution for pattern development. Remaining photoresist after pattern development acts as an etching protective layer. The sample was post-baked at 120 °C on a hot plate. The part of YBCO film, which was not covered with photo-resist, was then wet etched using 0.04% nitric acid. The sample was finally rinsed in acetone to remove the photoresist and dried with nitrogen flow. The optical image of the sample is shown in Figure 1(b).

2- Optical pump-Terahertz probe Measurements:

The terahertz transmission measurements were carried out using Optical-Pump-Terahertz-Probe (OPTP) setup that is based on ZnTe nonlinear terahertz generation and detection. Optical laser beam of pulse width of ~ 120 fs with a 1 kHz repetition rate was split into two parts with one being used for pumping the ZnTe crystal for terahertz generation-detection and the other part of the beam (800 nm, 1.55 eV) was used for optical excitation of superconducting YBCO metamaterial. The photoexcitation pulse has a photon energy (1.55 eV) much higher than the binding energy of the Cooper pairs (20-30 meV) present in the superconducting YBCO sample.[3-5] The optical pump beam has a beam diameter of approximately 10 mm, which is much larger than the focused terahertz beam spot size of nearly 4 mm at the sample position, providing a uniform photoexcitation over the YBCO-TASR sample. The time delay between optical-pump and terahertz-probe pulses was controlled by using a motorized delay stage and the delay is set to be 4.9 ps, where the dissociation of Cooper pairs is the maximum. At this pump-probe delay position (τ_p), the terahertz scan was performed on the sample and the reference substrate and later in the

post processing steps the spectrum through the sample ($E_S(\omega)$) is normalized to the reference substrate transmission spectra ($E_R(\omega)$) using the relation $|T(\omega)| = |E_S(\omega)|/|E_R(\omega)|$.

References:

[1] M. K. Wu, J. R. Ashburn, C. J. Torng, P. H. Hor, R. L. Meng, L. Gao, Z. J. Huang, Y. Q. Wang, and C. W. Chu, *Phys. Rev. Lett.* **1987**, *58*, 908.

[2] Z. X. Zhao, *Int. J. Mod. Phys. B*, **1987**, *1*, 179.

[3] S. D. Brorson, R. Buhleier, I. E. Trofimov, J. O. White, Ch. Ludwig, F. F. Balakirev, H.-U. Habermeier, and J. Kuhl, *J. Opt. Soc. Am. B*, **1996**, *13*, 1979.

[4] D. N. Basov and T. Timusk, *Rev. Mod. Phys.* **2005**, *77*, 721.

[5] T. Timusk, T. and B. Statt, *Rep. Prog. Phys.* **1999**, *62*, 61.

[6] R. A. Kaindl, M. Woerner, T. Elsaesser, D. C. Smith, J. F. Ryan, G. A. Farnan, M. P. McCurry, D. G. Walmsley, *Science*, **2000**, *287*, 470.

[7] R. D. Averitt, G. Rodriguez, A. I. Lobad, J. L. W. Siders, S. A. Trugman, and A. J. Taylor, *Phys. Rev. B*, **2001**, *63*, 140502(R).

[8] A. Dienst, M. Hoffmann, D. Fausti, J. Petersen, S. Pyon, T. Takayama, H. Takagi, A. Cavalleri, *Nat. Photon.* **2011**, *5*, 485.

[9] R. Singh, J. Xiong, A. K. Azad, H. Yang, S. A. Trugman, Q. X. Jia, A. J. Taylor, H.-T. Chen, *Nanophotonics*, **2012**, *1*, 117.

[10] M. Tonouchi, M. Tani, Z. Wang, K. Sakai, S. Tomozawa, M. Hangyo, Y. Murakami, and S. Nakashima, *Jpn. J. Appl. Phys.* **1996**, *35*, 2624.

[11] M. Tonouchi, M. Tani, Z. Wang, K. Sakai, M. Hangyo, N. Wada, and Y. Murakami, *IEEE Trans. Applied Superconductivity*, **1997**, *7*, 2913.

[12] J. B. Pendry, A. Holden, D. Robbins, and W. Stewart, *IEEE Trans. Microwave Theory Tech*, **1999**, *7*, 2075.

[13] D. R. Smith, W. J. Padilla, D. C. Vier, S. C. Nemat-Nasser, and S. Schultz, *Phys. Rev. Lett.* **2000**, *84*, 4184.

[14] J. B. Pendry, *Phys. Rev. Lett.* **2000**, *85*, 3966.

[15] N. I. Zheludev, S. L. Prosvirnin, N. Papasimakis, and V. A. Fedotov, *Nat. Photon.* **2008**, *2*, 351.

[16] S. Zhang, D. A. Genov, Y. Wang, M. Liu, and X. Zhang, *Phys. Rev. Lett.* **2008**, *101*, 047401.

[17] N. I. Landy, S. Sajuyigbe, J. J. Mock, D. R. Smith, and W. J. Padilla, *Phys. Rev. Lett.* **2008** *100*, 207402.

[18] V. M. Shalaev, *Nat. Photon.* **2007**, *1*, 41.

[19] S. M. Anlage, *J. Opt.* **2011**, *13*, 024001.

[20] G. Scalari, C. Maiseen, S. Cibella, R. Leoni, and J. Faist, *Appl. Phys. Lett.* **2014**, *105*, 261104.

[21] Y. K. Srivastava, and R. Singh, *J. Appl. Phys.* **2017**, *122*, 183104.

[22] R. Singh, and N. I. Zheludev, *Nat. Photon.* **2014***, 8*, 679.

[23] Y. K. Srivastava, M. Manjappa, H. N. S. Krishnamoorthy and R. Singh, *Adv. Opt. Mater.* **2016**, *4*, 1875.

[24] M. C. Ricci, H. Xu, R. Prozorov, A. P. Zhuravel, A. V. Ustinov, S. M. Anlage, *IEEE Trans. on Applied Superconductivity*, **2007**, *17*, 918.

[25] B. Jin, C. Zhang, S. Engelbrecht, A. Pimenov, J. Wu, Q. Xu, C. Cao, J. Chen, W. Xu, L. Kang, and P. Wu, *Opt. Express*, **2010**, *18*, 17504.

[26] D. Wang, Z. Tian, C. Zhang, X. Jia, B. Jin, J. Gu, J. Han and W. Zhang, *J. Opt.* **2014**, *16*, 094013.

[27] H-T. Chen, H. Yang, R. Singh, J. F. O'Hara, A. K. Azad, S. A. Trugman, Q. X. Jia, and A. J. Taylor, *Phys. Rev. Lett.* **2010**, *105*, 247402.

[28] J. Gu, R. Singh, Z. Tian, W. Cao, Q. Xing, M. He, J. W. Zhang, J. Han, H.-T. Chen, and W. Zhang, *Appl. Phys. Lett.* **2010**, *97*, 071102.

[29] V. A. Fedotov, A. Tsiatmas, J. H. Shi, R. Buckingham, P. de Groot, Y. Chen, S. Wang, and N. I. Zheludev, *Opt. Express,* **2010**, *18*, 9015.

[30] V. Savinov, V. A. Fedotov, S. M. Anlage, P. A. J. de Groot, and N. I. Zheludev, *Phys. Rev. Lett.* **2012**, *109*, 243904.

[31] C. Li, C. Zhang, G. Hu, G. Zhou, S. Jiang, C. Jiang, G. Zhu, B. Jin, L. Kang, W. Xu, J. Chen, and P. Wu, *Appl. Phys. Lett.* **2016***, 109*, 022601.

[32] C. Li, J. Wu, S. Jiang, R. Su, C. Zhang, C. Jiang, G. Zhou, B. Jin, L. Kang, W. Xu, J. Chen, and P. Wu, *Appl. Phys. Lett.* **2017,** *111***,** 092601**.**

[33] U. Fano, *Phys. Rev.* **1961**, *124*, 1866.

[34] A. E. Miroshnichenko, S. Flach, Y. S. Kivshar, *Rev. Mod. Phys.* **2010**, *82*, 2257.

[35] F. Hao, Y. Sonnefraud, P. V. Dorpe, S. A. Maier, N. J. Halas, P. Nordlander, *Nano Lett.* **2008**, *8*, 3983.

[36] B. Luk'yanchuk, N. I. Zheludev, S. A. Maier, N. J. Halas, P. Nordlander, H. Giessen, C. T. Chong, *Nat. Mater.* **2010**, *9*, 707.

[37] C. Wu, A. B. Khanikaev, R. Adato, N. Arju, A. A. Yanik, H. Altug, G. Shvets, *Nat. Mater.* **2012***, 11*, 69.

[38] V. Savinov, V. A. Fedotov, P. A. J. de Groot, and N. I. Zheludev, *Supercond. Sci. Technol.* **2013**, *26*, 084001.

[39] V. Savinov, K. Delfanazari, V. A. Fedotov, and N. I. Zheludev, *Appl. Phys. Lett.* **2016***, 108*, 101107.

[40] B. Xie, K. Tang, H. Cheng, Z. Liu, S. Chen, and J. Tian, *Adv. Mater.* **2017***, 29*, 1603507.

[41] Z. Li, W. Liu, H. Cheng, S. Chen, and J. Tian, *Sci. Rep.* **2015**, *5*, 18106.

[42] W. Liu, S. Chen, Z. Li, H. Cheng, P. Yu, J. Li, and J. Tian, *Opt. Lett.* **2015**, *40*, 3185.

[43] P. Yu, S. Chen, J. Li, H. Cheng, Z. Li, W. Liu, B. Xie, Z. Liu, and J. Tian, *Opt. Lett*. **2015**, *40*, 3229.

[44] J. Li, S. Chen, H. Yang, J. Li, P. Yu, H. Cheng, C. Gu, H-T Chen, and J. Tian, *Adv. Funct. Mater.* **2015**, *25*, 704.

[45] P. Yu, J. Li, C. Tang, H. Cheng, Z. Liu, Z. Li, Z. Liu, C. Gu, J. Li, S. Chen, and J. Tian, *Light Sci. Appl.* **2016**, *5*, e16096.

[46] Z. Liu, Z. Li, Z. Liu, J. Li, H. Cheng, P. Yu, W. Liu, C. Tang, C. Gu, J. Li, S. Chen, and J. Tian, *Adv. Funct. Mater.*, **2015**, *25*, 5428.

[47] H. Cheng, Z. Liu, S. Chen, and J. Tian, *Adv. Mater.* **2015**, *27*, 5410.

[48] J. Li, P. Yu, H. Cheng, W. Liu, Z. Li, B. Xie, S. Chen, and J. Tian, *Adv. Opt. Mater.* **2016**, *4*, 91.

[49] Z. Li, W.Liu, H. Cheng, S. Chen and J. Tian, *Sci. Rep.* **2017**, *7*, 8204.

[50] R. Singh, I. Al-Naib, M. Koch, and W. Zhang, *Opt. Express,* **2011**, *19*, 6312

[51] L. Cong, M. Manjappa, N. Xu, I. Al-Naib, W. Zhang, and R. Singh, *Adv. Opt. Mater.* **2015**, *3*, 1537.

[52] Y. K. Srivastava, M. Manjappa, L. Cong, W. Cao, I. Al-Naib, W. Zhang, R. Singh, *Adv. Opt. Mater.* **2016**, *4*, 457.

[53] M. Khorasaninejad, W. T. Chen, R. C. Devlin, J. Oh, A. Y. Zhu, F. Capasso, *Science,* **2016,** *352*, 1190.

[54] Q. Wang, E. T. F. Rogers, B. Gholipour, C.-M. Wang, G.Yuan, J. Teng and N. I. Zheludev, *Nat. Photon.* **2016***,10*, 60.

[55] Y. Xu, "Optical Studies of Ultrafast Carrier Dynamics in High Temperature Superconductors", Ph.D. Thesis, University of Rochester, **2004**.

[56] W. Li, C. Zhang, X. Wang, J. Chakhalian, and M. Xiao, *J. Magn. Magn. Mater.* **2015**, *376*, 29.

[57] M. C. Ricci and S. M. Anlage, *Appl. Phys. Lett.* **2006**, *88*, 264102.

[58] J. Zhou, Th. Koschny, M. Kafesaki, E. N. Economou, J. B. Pendry, and C. M. Soukoulis, *Phys. Rev. Lett.* **2005**, *95*, 223902.

Figure 1

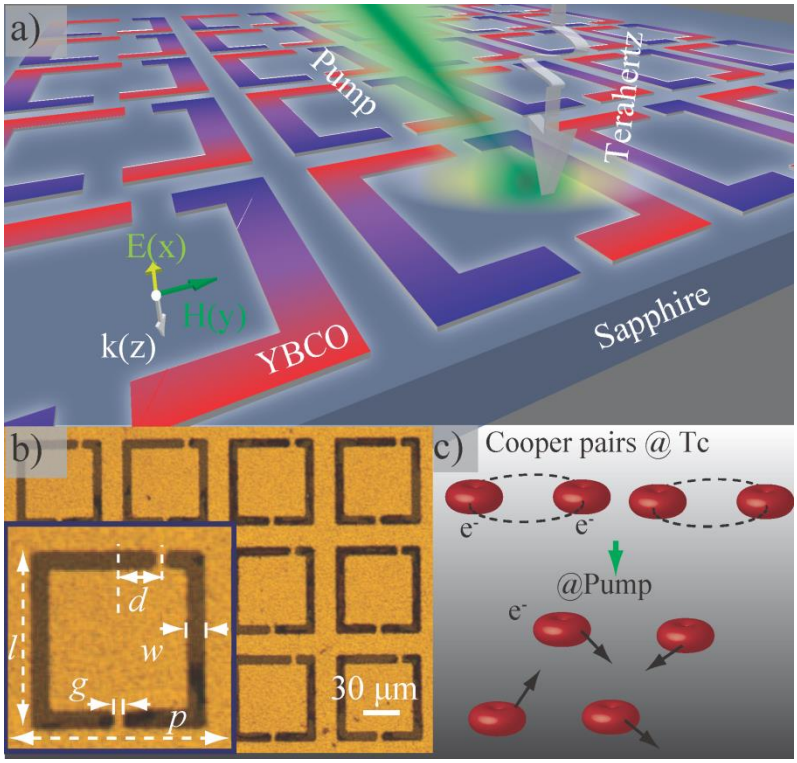

Figure 1: Schematic diagram of the asymmetric metamaterial array. (a) The artistic illustration of the OPTP measurements on the YBCO metamaterials; (b) optical image of the fabricated metamaterial sample (YBCO-TASR) with inset depicting the geometrical dimensions of a unit cell with resonator length, *l*: 60 µm; asymmetry distance, *d*: 15 µm, gap *g*: 3 µm, resonator width, *w*: 6 µm and the periodicity, *p*: 75 µm. (c) Schematic illustration of Cooper pairs dissociating into quasiparticles due to excitation with optical pump.

Figure 2

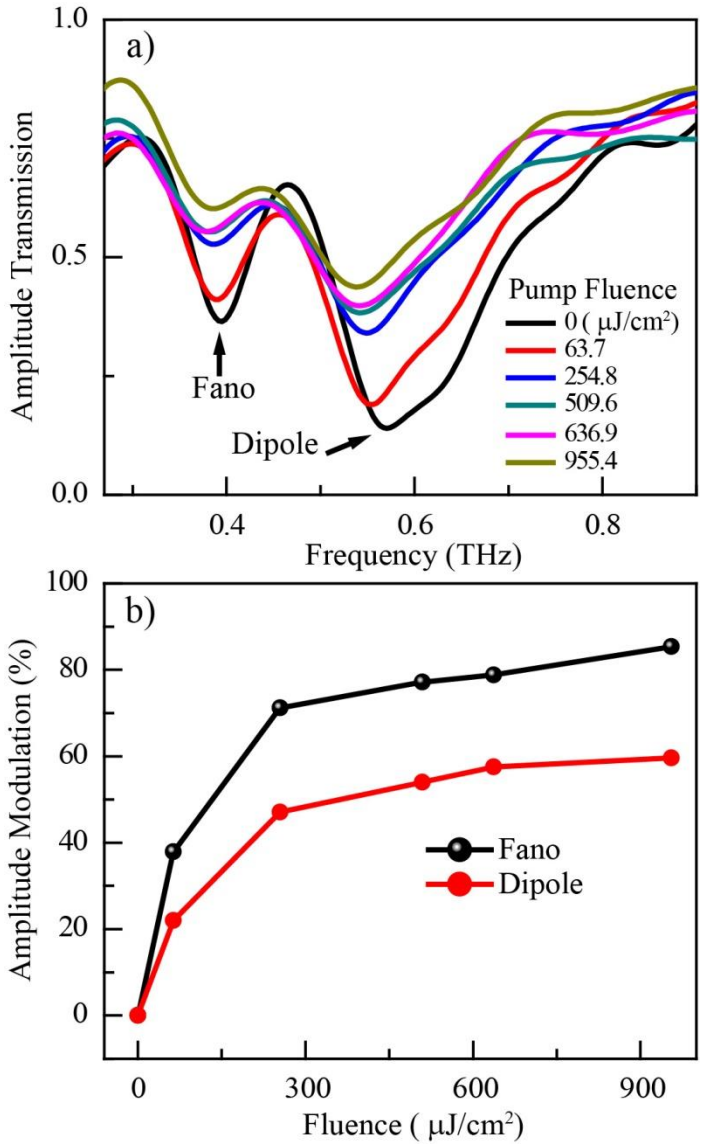

Figure 2: (a) The amplitude transmission spectra of YBCO-TASR for varying fluences of incident pump beam of 800 nm wavelength. (b) The amplitude modulation depth of Fano and dipole resonances with respect to the increasing fluences of pump beam.

Figure 3

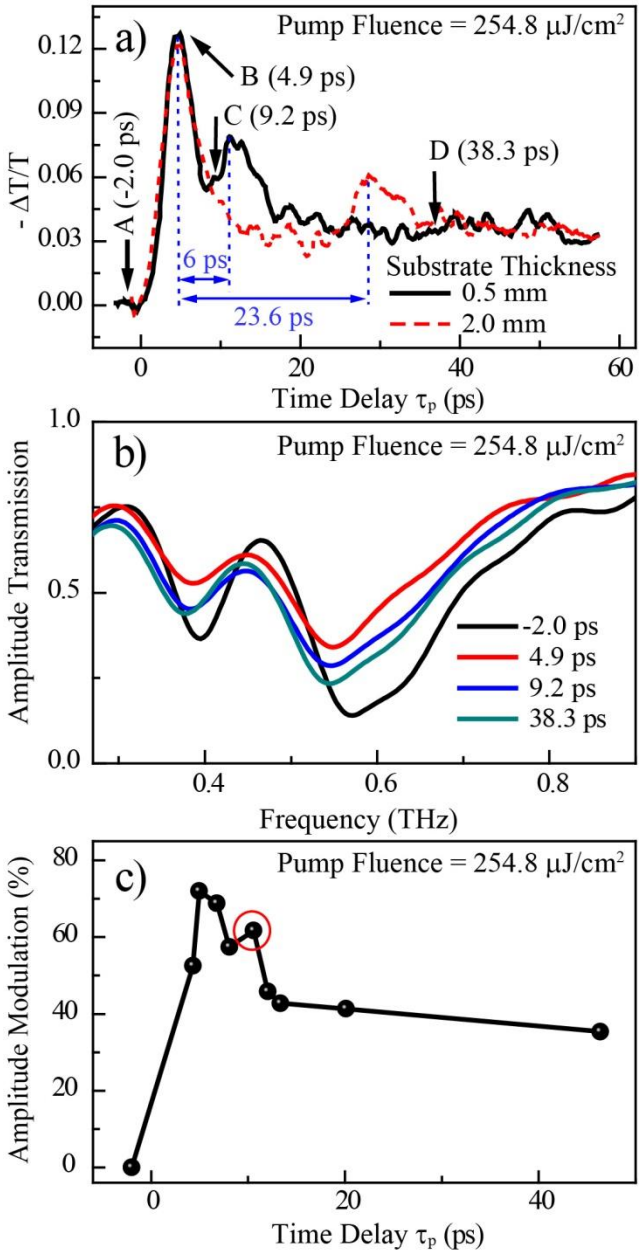

Figure 3: (a) Charge carrier dynamics of the YBCO-TASR performed using the time-resolved OPTP measurements for the pump fluence of 254.8 μJ/cm^2. Red dashed curve indicates the charge carrier dynamics of the YBCO-TASR fabricated over 2 mm thick sapphire substrate. (b) The amplitude transmission spectra at different pump-probe time delays. (c) The amplitude modulation of the Fano resonance for varying pump probe time delays.

Figure 4

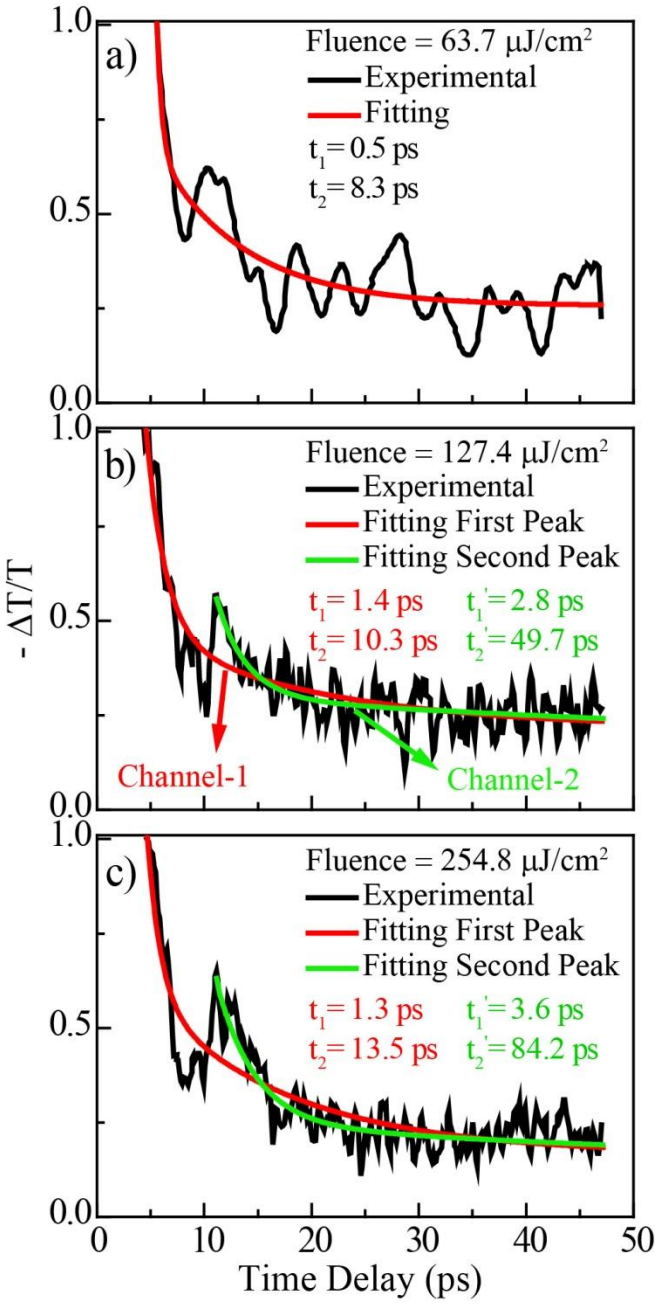

Figure 4: Normalized charge carrier relaxation dynamics of the YBCO-TASR performed using the time-resolved OPTP measurements at excitation pump fluences (a) 63.7 μJ/cm^2, (b) 127.4 μJ/cm^2 and (c) 254.8 μJ/cm^2. Red and green line depicts the fitting of recombination dynamics using bi-exponential decay for first and second peak, respectively.

Figure 5

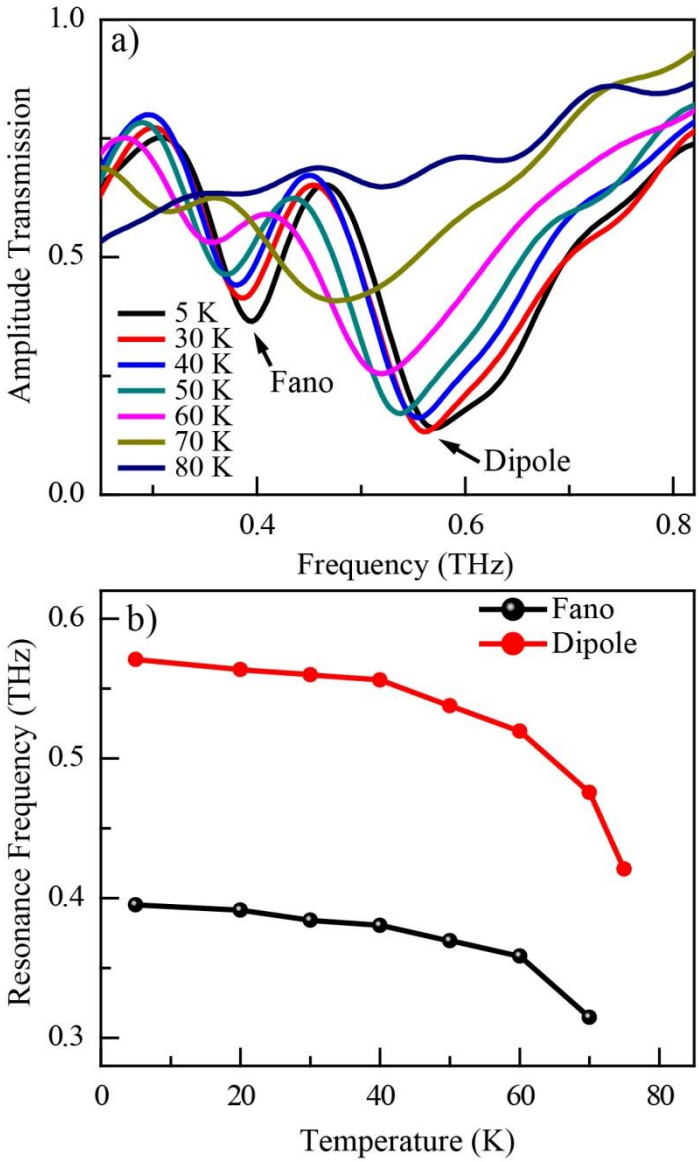

Figure 5: (a) The amplitude transmission spectra of YBCO-TASR at different temperatures ranging from 5 K to 80 K. The incident electric field is polarized perpendicular to the split gaps. (b) The frequency shift of Fano and dipole resonance at different temperatures.